NSTX

Supported by

U.S. DEPARTMENT OF ENERGY | Office of Science

Comparison of poloidal velocity measurements to neoclassical theory on NSTX

College W&M
Colorado Sch Mines
Columbia U
CompX
General Atomics
INL
Johns Hopkins U
LANL
LLNL
Lodestar
MIT
Nova Photonics
New York U
Old Dominion U
ORNL
PPPL
PSI
Princeton U
Purdue U
SNL
Think Tank, Inc.
UC Davis
UC Irvine
UCLA
UCSD
U Colorado
U Illinois
U Maryland
U Rochester
U Washington
U Wisconsin

Ronald E. Bell

Princeton Plasma Physics Laboratory

In collaboration with
R. Andre, S. M. Kaye, R. A. Kolesnikov, B. P. LeBlanc, G. Rewoldt, S. A. Sabbagh, W. X. Wang

51st Annual Meeting of the Division of Plasma Physics
Atlanta, GA
November 2-6, 2009

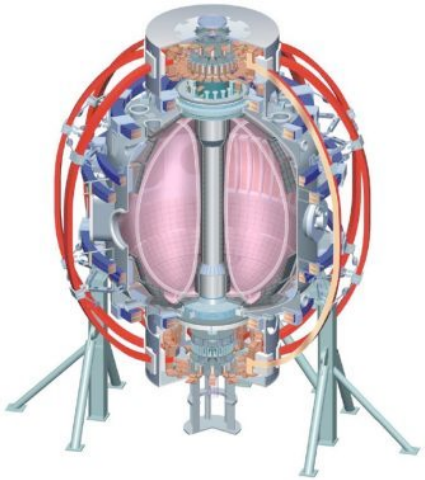

Culham Sci Ctr
U St. Andrews
York U
Chubu U
Fukui U
Hiroshima U
Hyogo U
Kyoto U
Kyushu U
Kyushu Tokai U
NIFS
Niigata U
U Tokyo
JAEA
Hebrew U
Ioffe Inst
RRC Kurchatov Inst
TRINITI
KBSI
KAIST
POSTECH
ASIPP
ENEA, Frascati
CEA, Cadarache
IPP, Jülich
IPP, Garching
ASCR, Czech Rep
U Quebec

Motivation

- Knowledge of poloidal velocity is required to determine E_r through the force balance equation
- Turbulence suppression and transport barrier formation are linked to E_r and ∇E_r
- Motional Stark Effect diagnostic needs E_r to obtain accurate pitch angle measurements
- Recent poloidal velocity measurements (JET, DIII-D) differ an order of magnitude from neoclassical estimates
- Advantageous to study poloidal flow on ST, low B field minimizes a dominant atomic physics issue
- Optimal symmetric viewing geometry on NSTX further reduces reliance on atomic physics

Outline

- Issues with poloidal velocity measurements
- Diagnostics
- Measurements
  - Line Integrated
  - Local after inversion
- Comparison with Neoclassical Theory
- Summary

Charge Exchange Recombination Spectroscopy

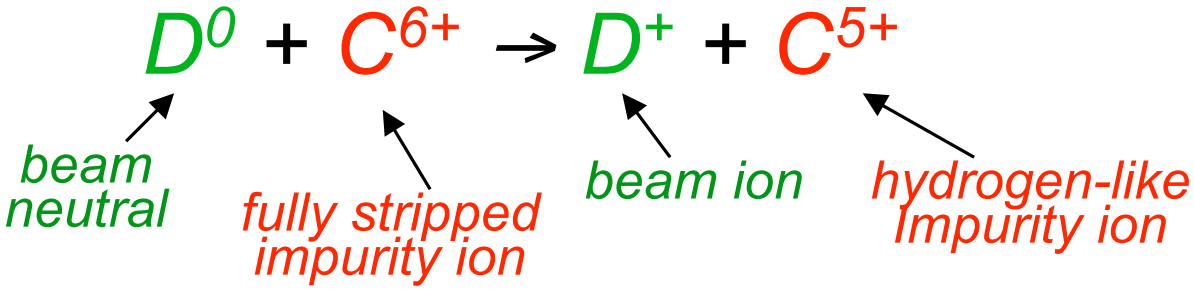

- $E_{CX} \propto n_{beam} n_{carbon} \langle \sigma v \rangle_{CX}$
- Charge exchange cross section varies with:
  - Full, half and third energy deuterium beam neutrals
  - Ground state (n=1) and excited neutrals (n≥2)
  - Ion temperature, toroidal velocity, Z_{eff}
- Desire flow measurement of fully stripped impurity, C^{6+}
- CX measurements of hydrogen-like ion, C^{5+} (n=8-7) 529 nm
- Competition from passive emission of C^{5+}
- C^{5+} product ions re-excited after prompt emission (plume)

Challenges of poloidal flow measurements

- Practical Issues
  - V_θ << V_ϕ, need precise alignment of viewing chords (< few arc minutes)
  - Finite height of neutral beam (non-local measurements)
- Issues associated with charge exchange recombination spectroscopy
  - Contributions from non-CX emission (intrinsic background, plume)
  - Energy dependent cross section adds velocity components not associated with plasma flow, scale with T_i
  - Uncertainty in rates for charge exchange,
    especially for 1/2 and 1/3 energy components
  - Large attenuation of beam neutrals
    (diminished signal in core)
  - Excitation of beam neutrals
    (small fraction with very large CX cross section)

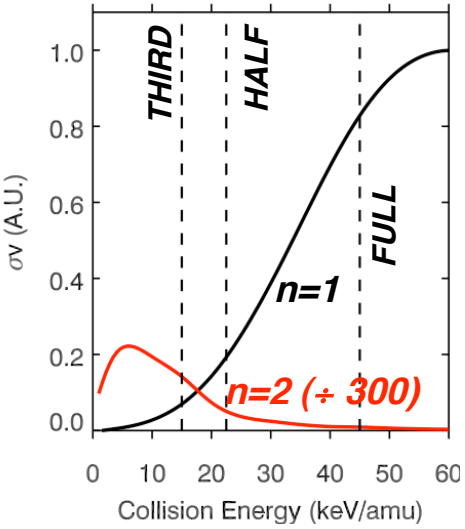

  - Gyro orbit finite lifetime effects (proportional to T_i and B) in plane of gyro orbit
  - Uncertainty in completeness of atomic physics treatment

Energy Dependent CX cross section results in net flow toward neutral beam

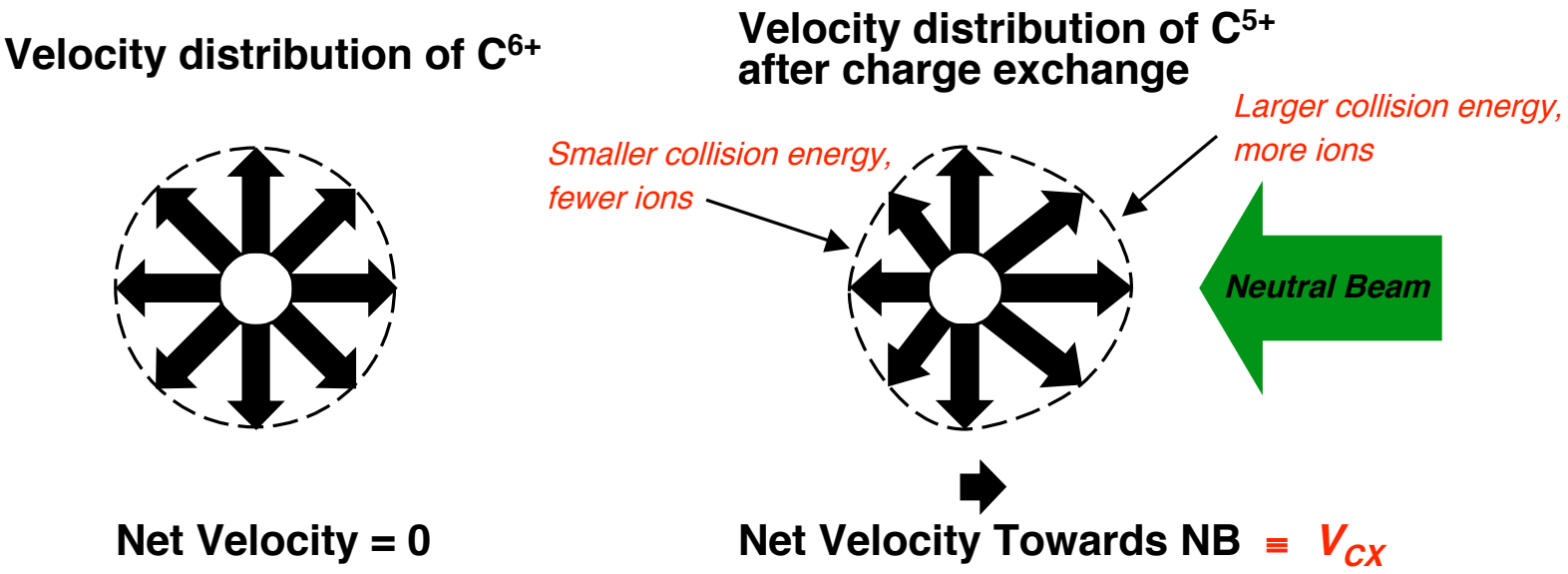

- After charge exchange, the population of C^{5+} ion have a net flow directed toward the beam
- This is a *real velocity* of the product ion, C^{5+}, that scales with T_i, and is additive to the velocity of the parent ion, C^{6+}
- The apparent velocity of the C^{5+} ion is view dependent
- All relevant atomic physics is encapsulated in this net flow toward beam

Gyro orbit finite lifetime effects scale with T_i and B

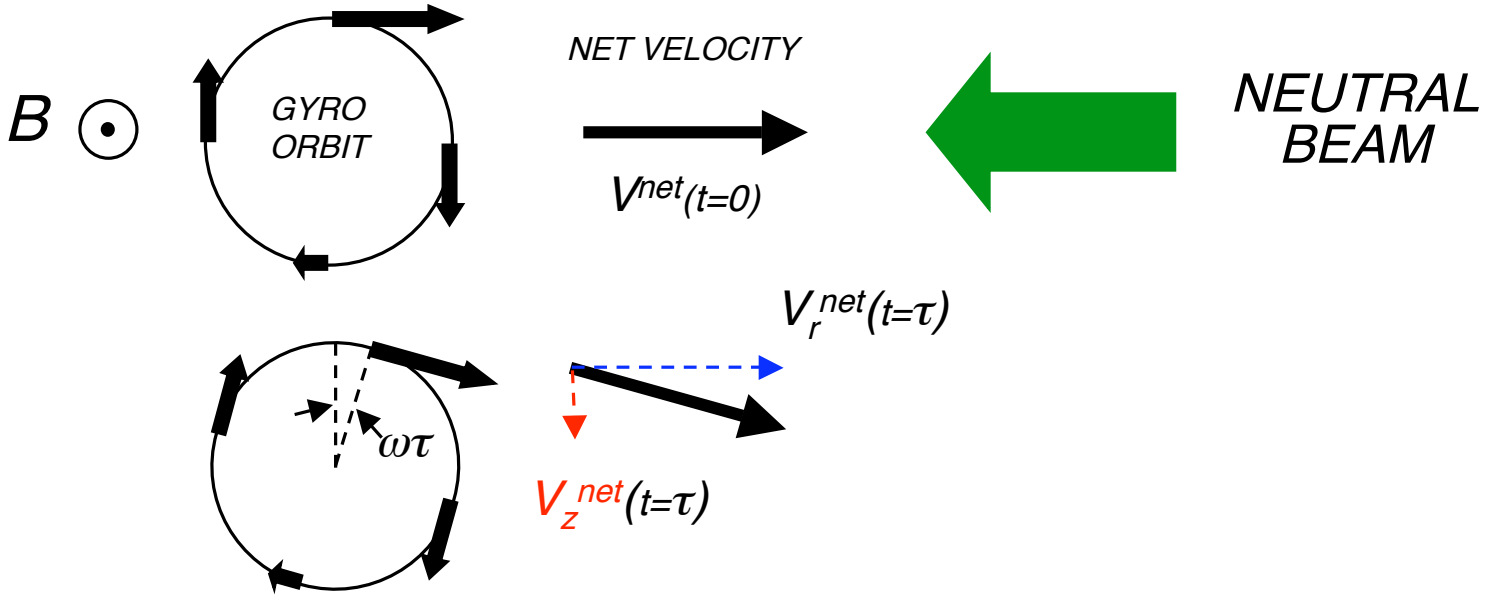

- Collision energy varies with gyro angle
- Ion precesses around gyro orbit by $\omega\tau$ before radiating
- Some of the net flow toward the beam (V_{CX}) is directed vertically
- Gyrofrequency $\omega \propto B$, $V_{CX} \propto T_i$, $\tau \approx 1$ ns
- $V_{gfl} \approx \omega\tau\, V_{CX} \propto T_i B$
- For TFTR: T_i = 30 keV, B = 5 T, $\omega\tau = 0.25$, $V_{gfl} \approx$ 40 km/s !
- For NSTX: $T_i \leq$ 3 keV, B = 0.3-0.5 T, $\omega\tau \approx 0.02$, $V_{gfl} \leq$ 0.3 km/s

Up/Down Symmetric Active and Passive Views Designed for Differential Velocity Measurements

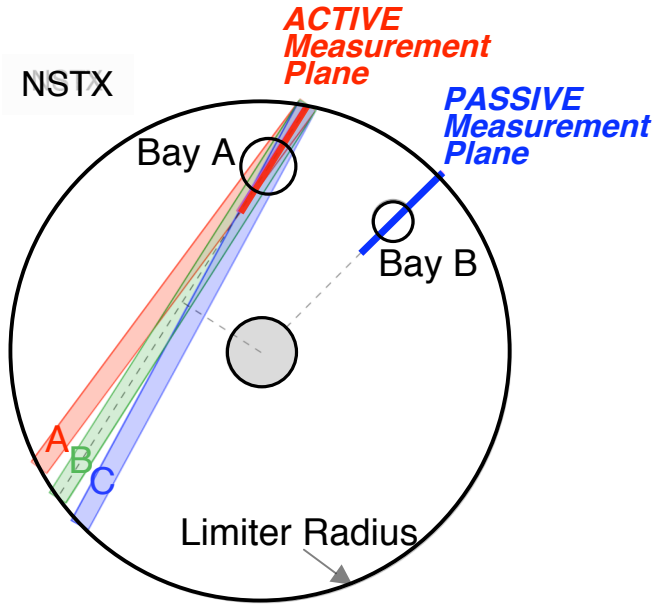

- Vacuum vessel designed with ports aligned with NBs
- Active plane parallel to NB, simultaneous passive measurement
- Eight lenses at 4 locations for 276 views
- 75 active, 63 passive differential velocity measurements
- Up/Down pairs precisely aligned at midplane

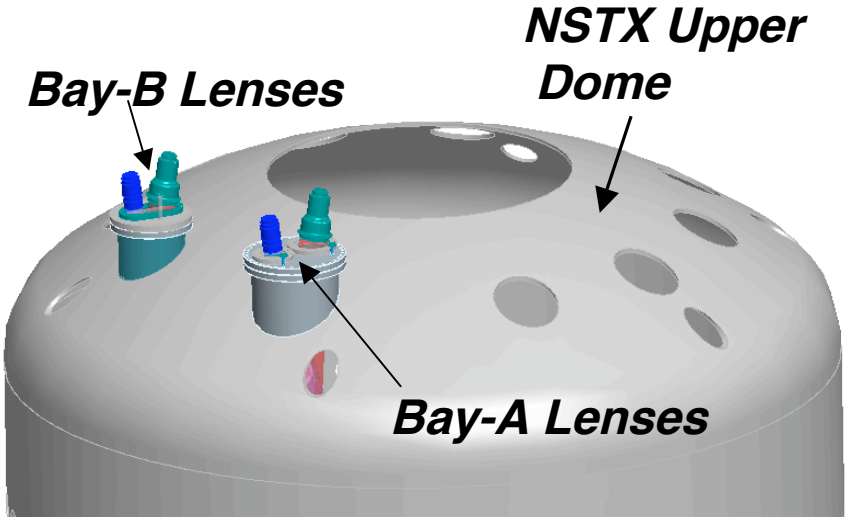

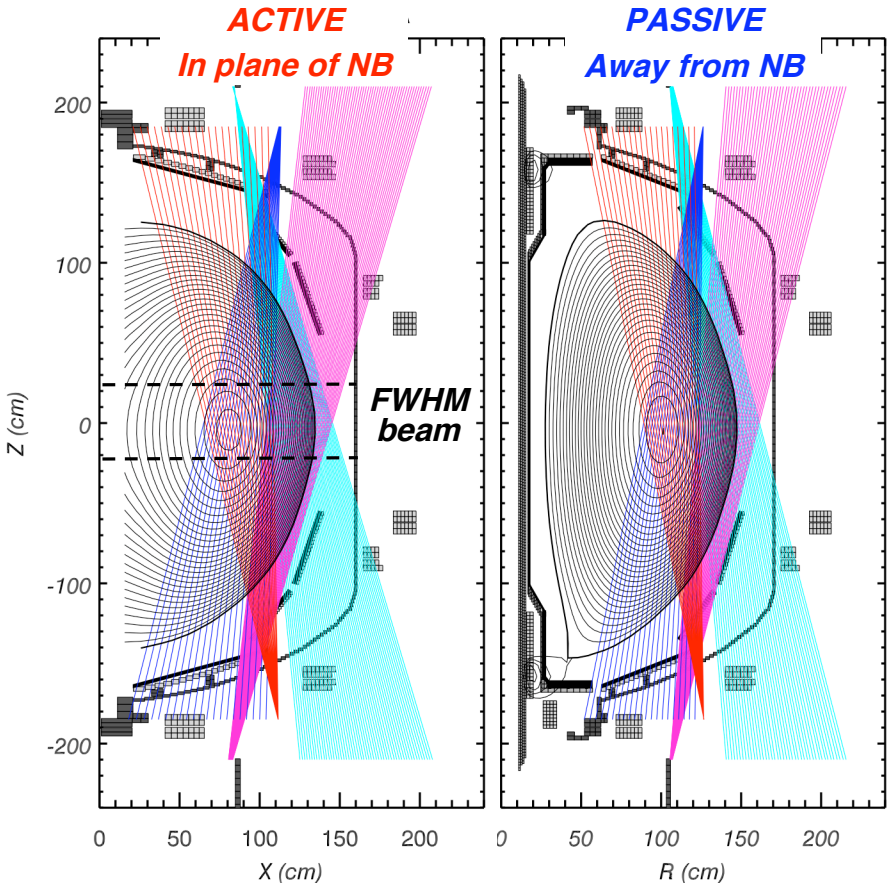

Differential Measurements Remove Non-Poloidal Velocity Components

$$\vec{v} = \vec{v}_\theta + \vec{v}_\phi + \vec{v}_{CX} + \vec{v}_{gfl}$$

Locally:

$$v^+_{app} = \hat{s}^+ \cdot \vec{v} = v_\theta + \alpha_1 v_\phi + \alpha_2 v_{cx} + \beta v_{gfl}$$

$$v^-_{app} = \hat{s}^- \cdot \vec{v} = -v_\theta + \alpha_1 v_\phi + \alpha_2 v_{cx} - \beta v_{gfl}$$

$$v_{diff} = \frac{1}{2}\left(v^+_{app} - v^-_{app}\right) = v_\theta + \beta v_{gfl} \approx v_\theta$$

$$\alpha_1 = \hat{s} \cdot \hat{\phi}$$

$$\alpha_2 = \hat{s} \cdot \hat{n}$$

$$\beta = \hat{n} \times \frac{\vec{B}}{|B|}$$

$v_{gfl} \approx \omega\tau v_{cx}$ (small < 0.3 km/s)

Use plasma symmetry for cancellation along line-integral:

$$u_{diff} = \frac{1}{2}\left(\frac{\int E_{CX} v^+ d\ell}{\int E_{CX} d\ell} - \frac{\int E_{CX} v^- d\ell}{\int E_{CX} d\ell}\right)$$

Multi-spectral imaging of both upper and lower views on detector improve measurement accuracy

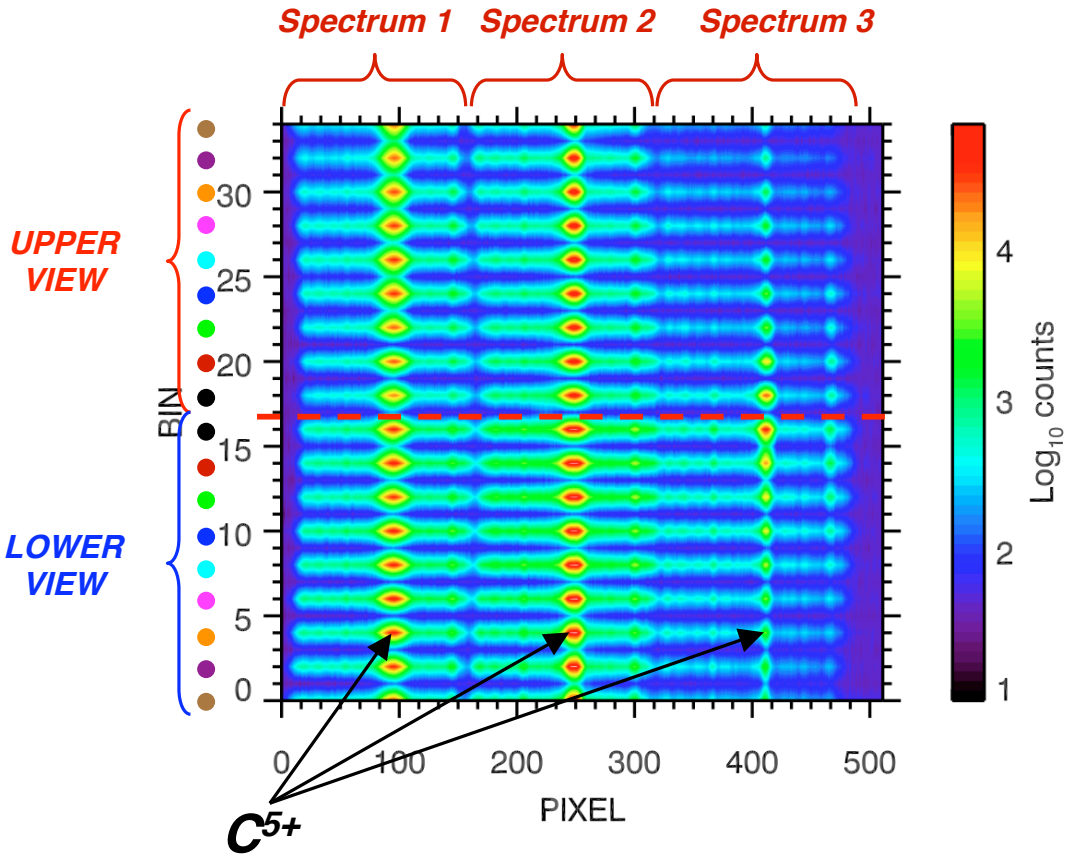

Raw data for one of 6 CCD detectors,10 ms integration time (Log scale)

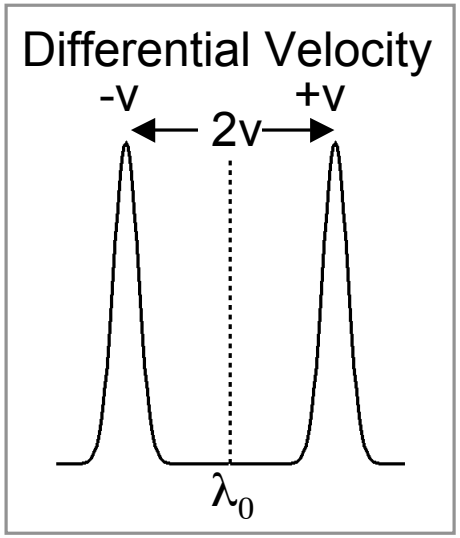

- Views from upper and lower ports are positioned symmetrically on each detector to improve accuracy of relative wavelength shifts
- Each pair makes an independent differential velocity measurement
- *Do not need precise rest wavelength!*
- *Insensitive to variance in λ calibration or changes in index of refraction of air*

Poloidal velocity measurements are supported by other diagnostics and systems

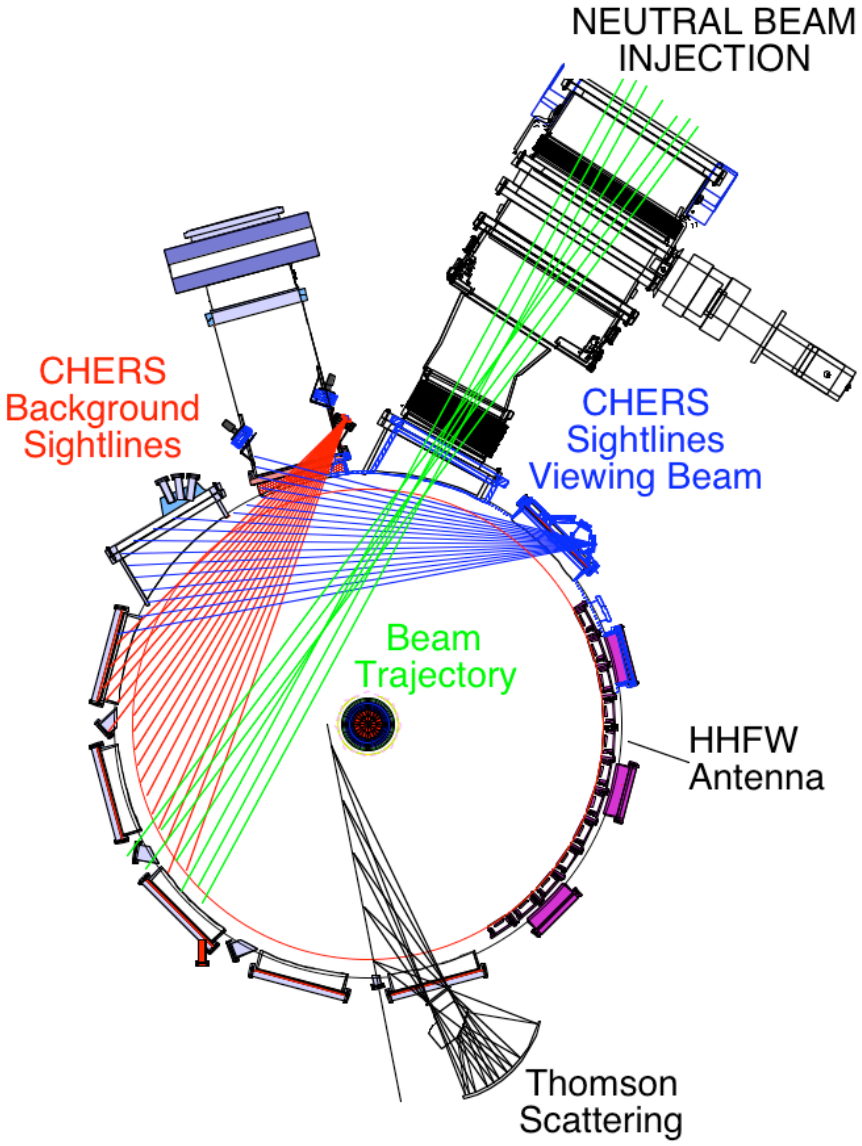

- NBI:
  - 80-90 kV, deuterium
  - 3 Sources
  - 6 MW
- Thomson Scattering:
  - $T_e(R,t)$, $N_e(R,t)$
  - 30 ch., 60 Hz
- Toroidal CHERS:
  - $T_i(R,t)$,$V_\phi(R,t)$, $N_c(R,t)$
  - 51ch., 10 ms
  - Δr = 0.5-3 cm
- Poloidal CHERS:
  - $V_\theta(R,t)$
  - 75 ch., 10 ms
  - Δr = 0.6-1.6 cm (after inversion)
- EFIT: Equilibrium reconstruction

Typical NSTX parameters for poloidal velocity measurements

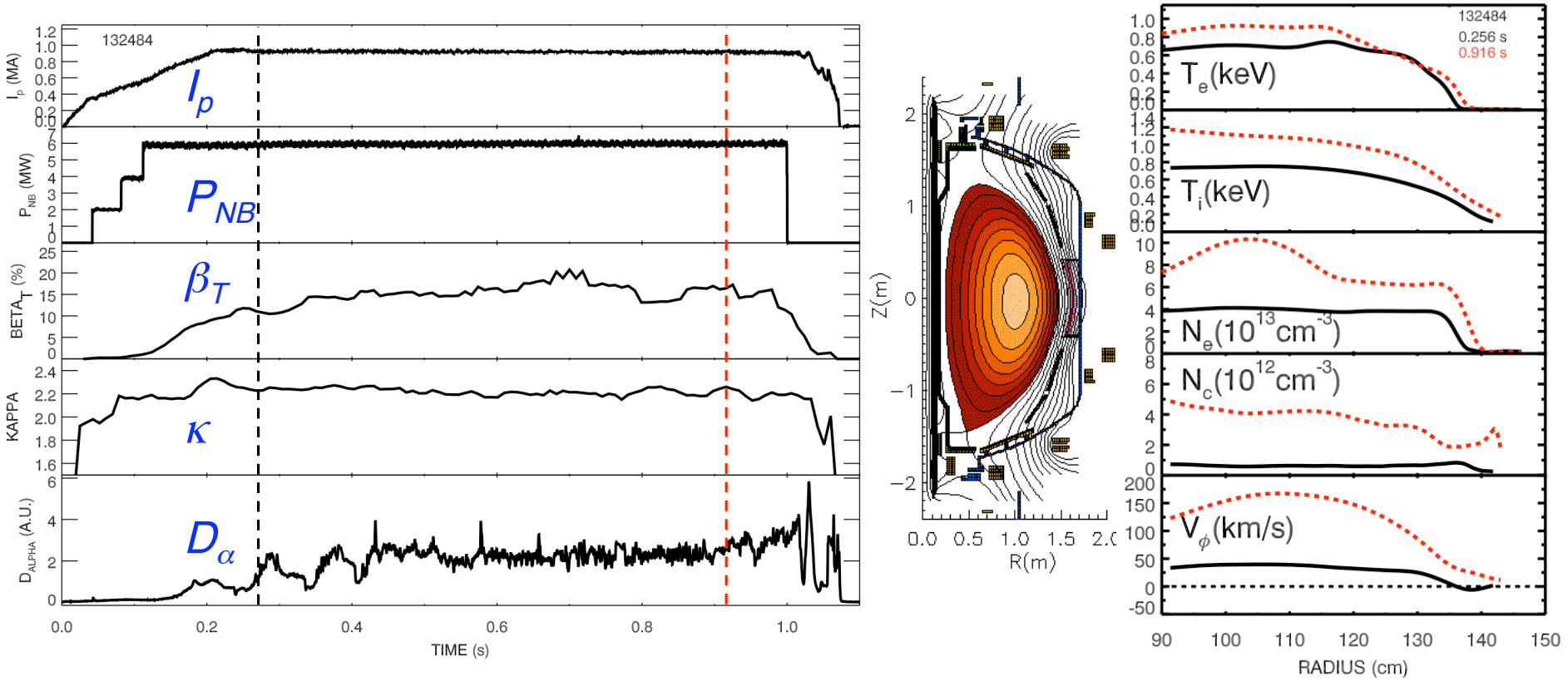

- Similar class of discharges examined here with variations in I_p and B as noted
- P_{NB} = 4, 6 MW, I_p = 0.7-1.1 MA, B = 0.34-0.54 T
- Initially compare early and late time with largely different profiles

Line-integrated Measurements of Brightness and Differential Velocity

Profiles of Brightness and line-integrated velocity from Active View across NB

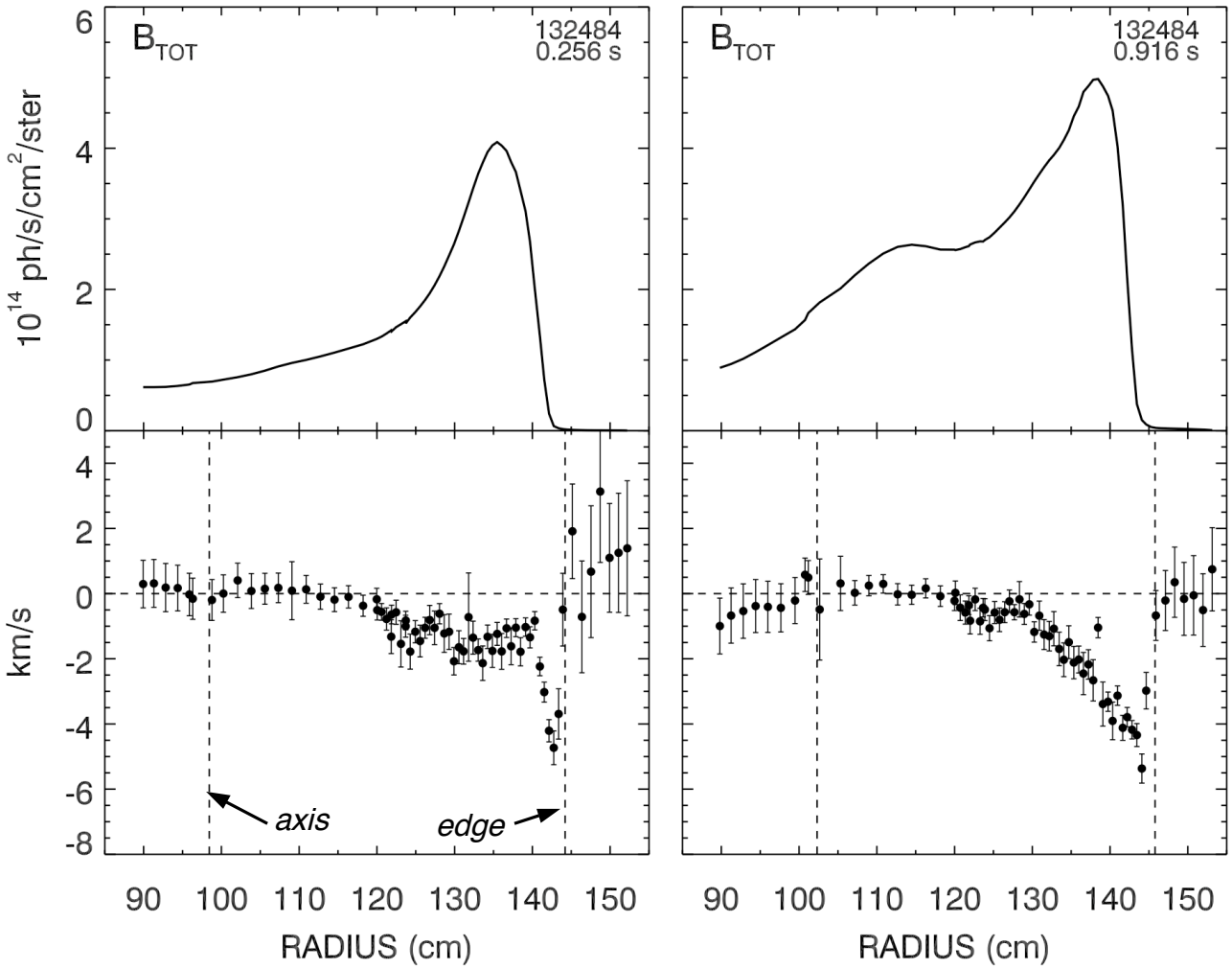

Apparent velocity, ACTIVE + PASSIVE

No atomic physics used here

Line-integrated Measurements of Brightness and Differential Velocity

A smoothing spline is fit to the data, shaded area shows uncertainty in spline fit

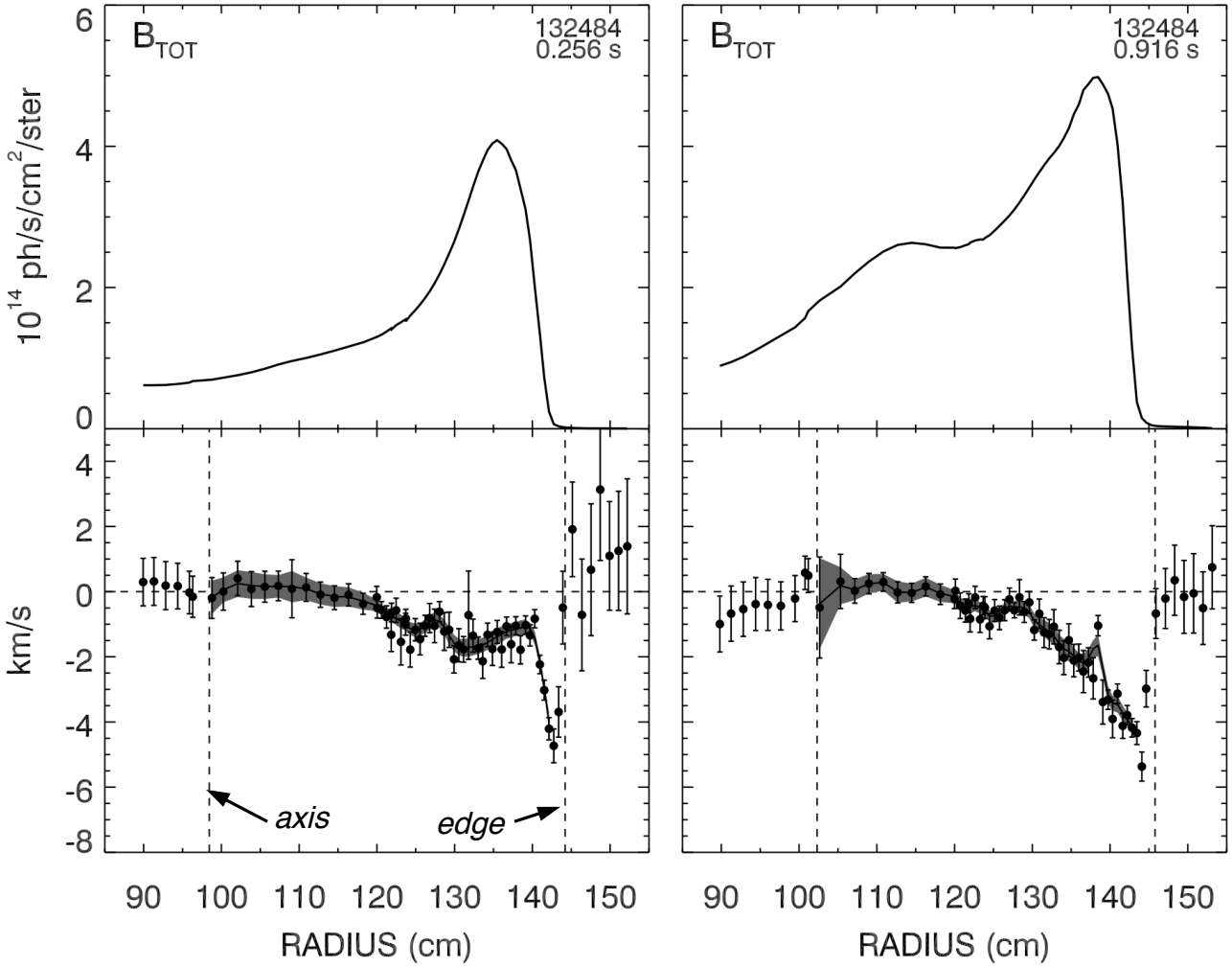

Apparent velocity, ACTIVE + PASSIVE

No atomic physics used here

Line-integrated Measurements of Brightness and Differential Velocity

Apparent velocity from Background emission is evaluated from Passive View

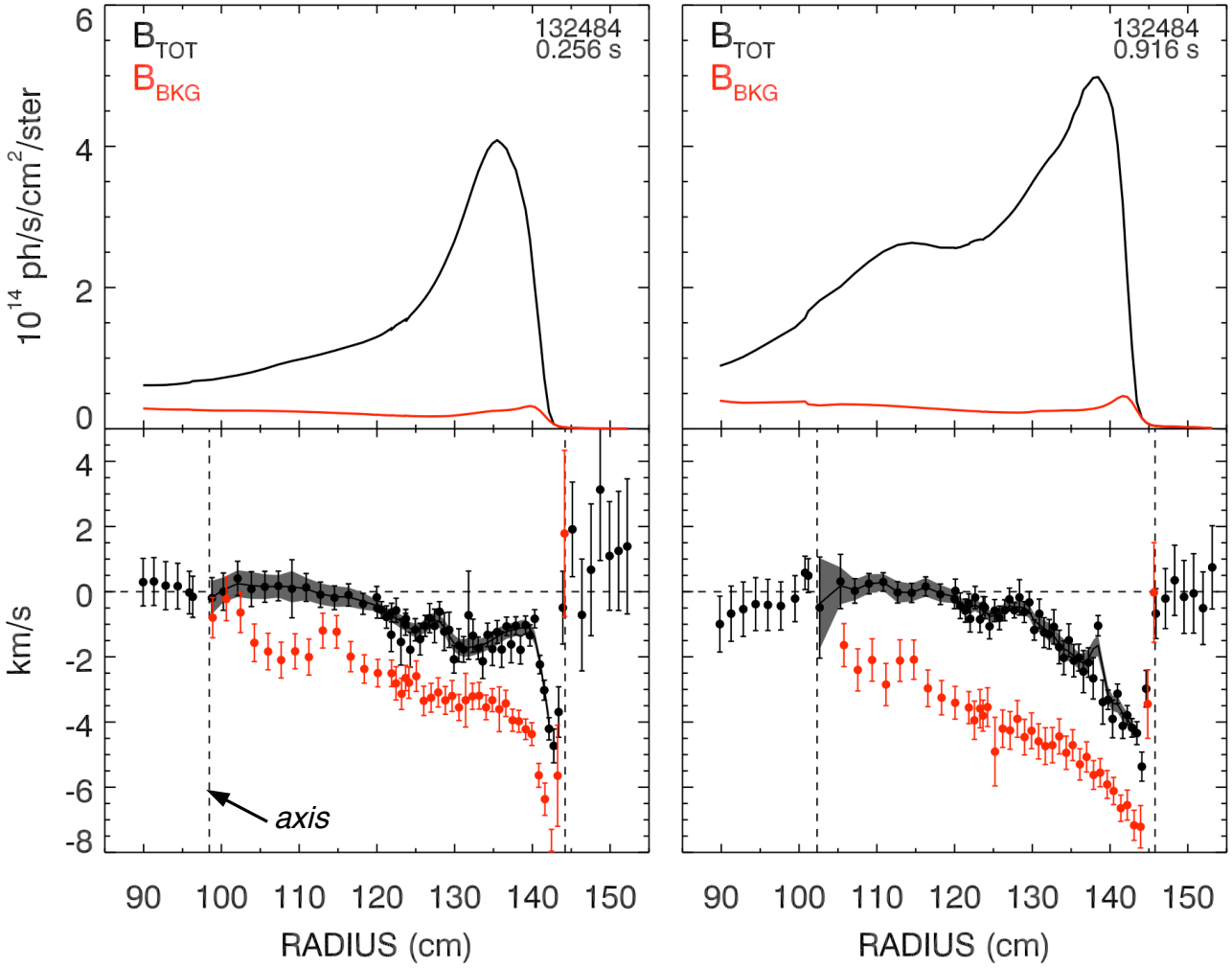

Apparent velocity, PASSIVE

No atomic physics used here

Line-integrated measurements of Brightness and Differential Velocity

Apparent velocity from CX emission alone is determined using relative brightnesses

$$B_{TOT}u_{TOT} = B_{CX}u_{CX} + B_{BKG}u_{BKG}$$

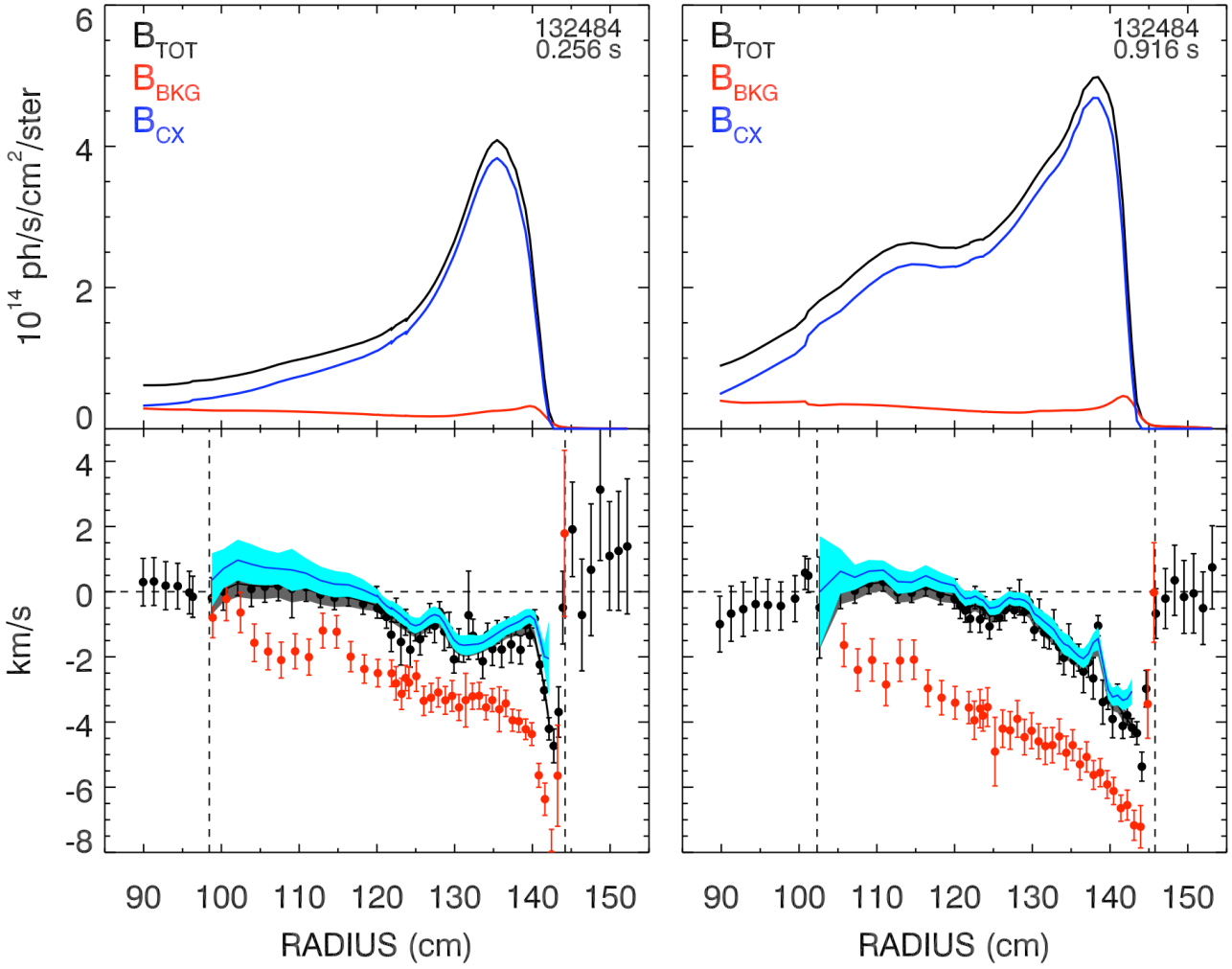

Apparent velocity, ACTIVE

No atomic physics used here

Finite Neutral Beam Height causes radial smearing

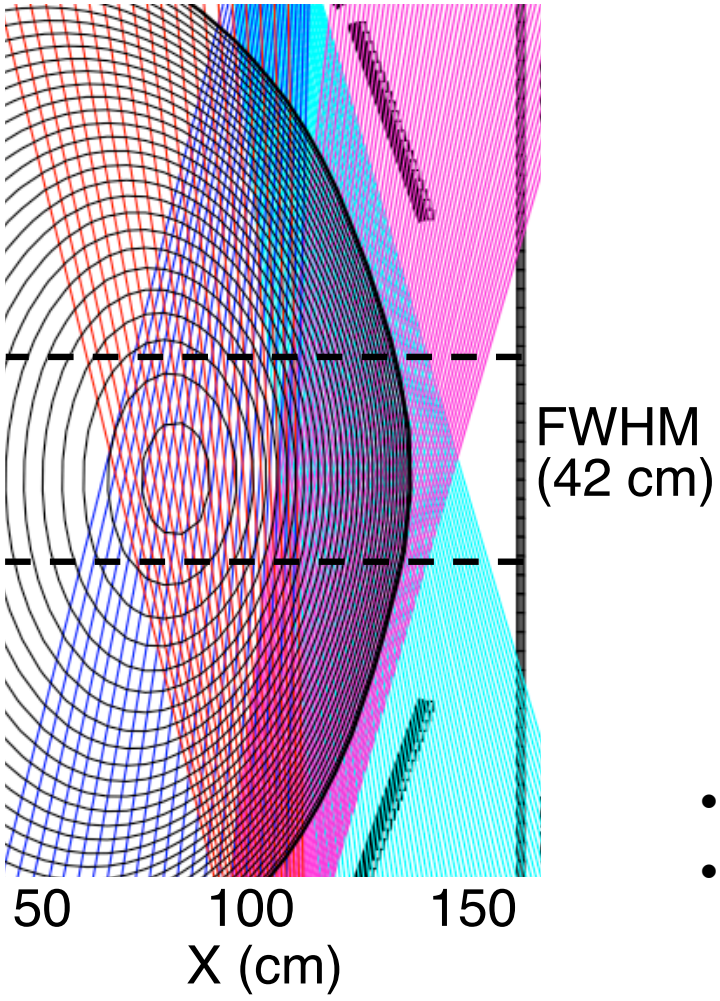

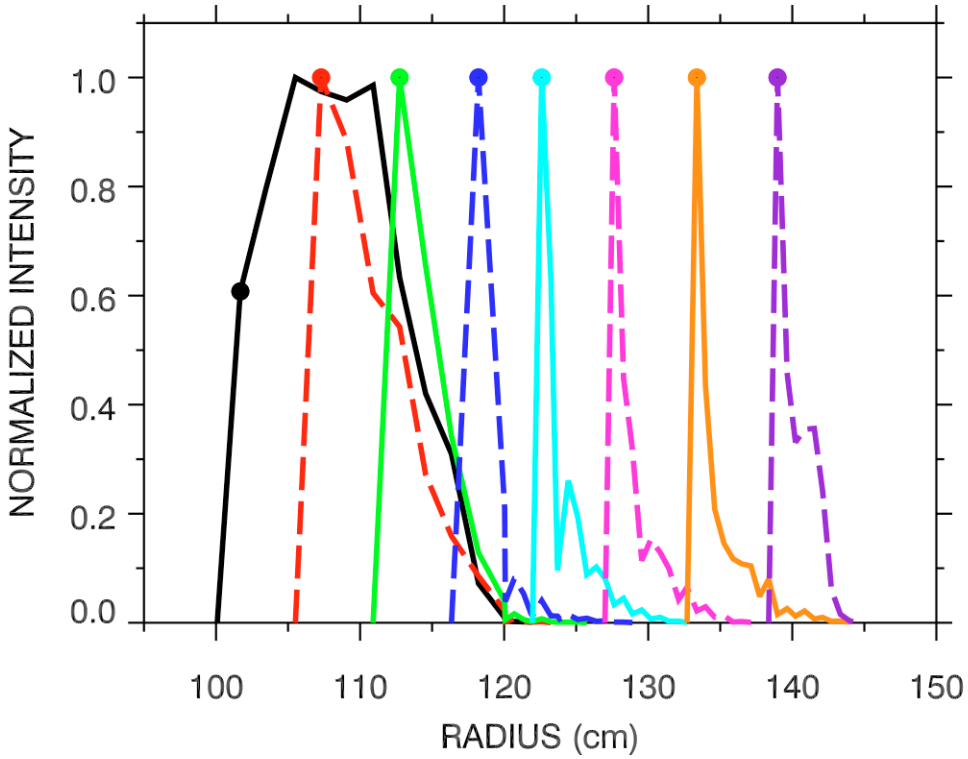

- Amount of radial smearing is plasma dependent
- Smearing varies across profile, worse near axis

Matrix Inversion of Passive Emission

$$4\pi B_i = \sum_j L_{ij} E_j \qquad E_j = 4\pi \sum_j L_{ji}^{-1} B_i$$

$$4\pi B_i u_i = \sum_j L_{ij} E_j \left(\hat{s}_i \cdot \vec{v}_j\right) = \sum_j L_{ij} E_j v_j \cos\theta_{ij}$$

$$M_{ij} \equiv L_{ij}\left(\hat{s}_i \cdot \hat{v}_j\right) = L_{ij}\cos\theta_{ij}$$

$$v_j = \frac{E_j v_j}{E_j} = \frac{\sum_i M_{ji}^{-1} B_i u_i}{\sum_j L_{ji}^{-1} B_i}$$

i - sightline

j - zone

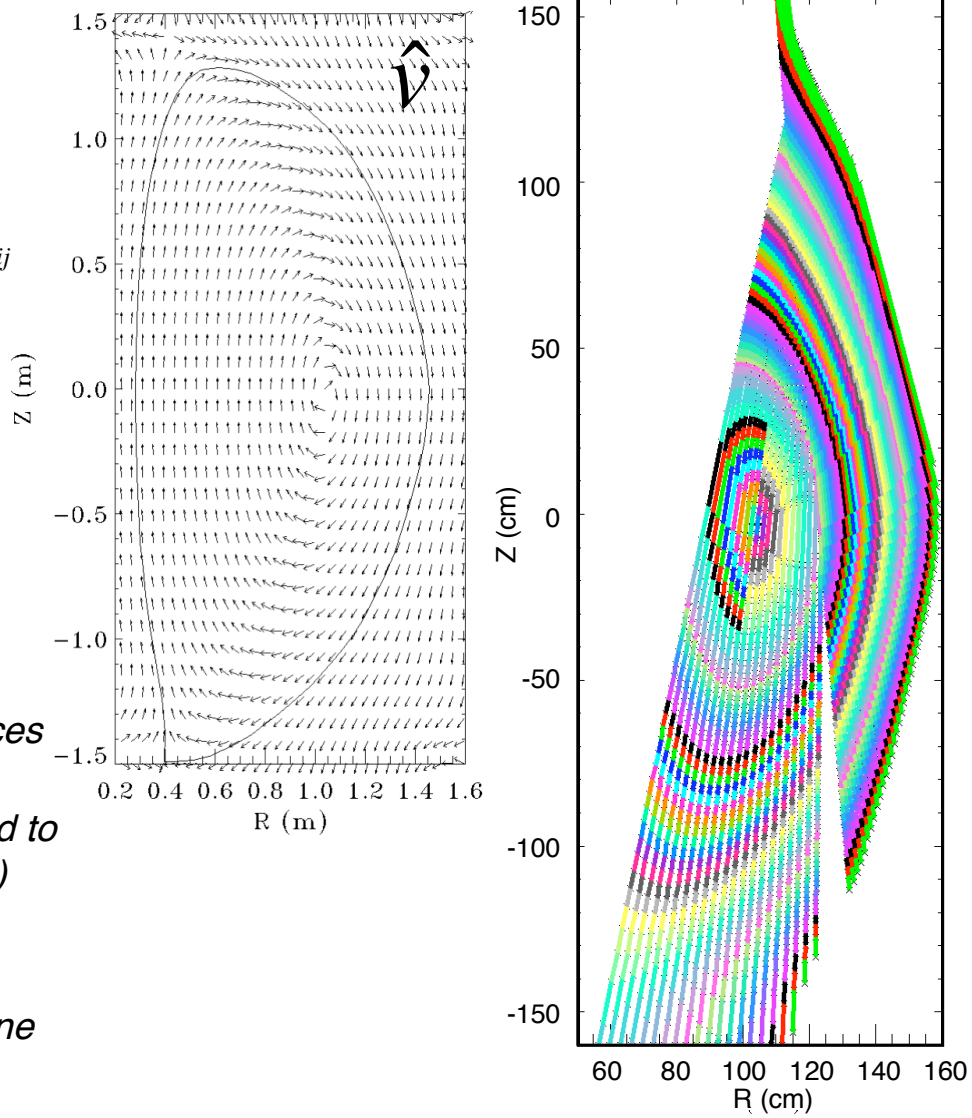

- *EFIT equilibrium is used to compute inversion matrices for passive emission*
- *Measured Brightness along a sightline can be related to local emissivity (assumed constant on a flux surface)*
- *The inverted velocity is obtained using two matrix inversions*
- *Brightness weighted velocity calculated in active plane geometry for subtraction of passive contributions*

Matrix Inversion of Active Emission to obtain local poloidal velocity

$$W_{ijk} = E_{ijk}^{CX} = n_j^C n_{jk}^{beam} \left\langle \sigma^{CX} v \right\rangle_{ijk}^{eff}$$

$$L_{ij} = \sum_k L'_{ijk}$$

$$2\pi\left(B_i u_i^{UP} - B_i u_i^{DOWN}\right) = \sum_{j,k} L'_{ijk} W_{ijk} v_j \cos\theta_{ijk}$$

$$P_{ij} \equiv \sum_k L'_{ijk} W_{ijk}$$

$$Q_{ij} \equiv \sum_k L'_{ijk} W_{ijk} \cos\theta_{ijk}$$

$$4\pi B_i = \sum_{j,k} L'_{ijk} W_{ijk} = \sum_{j,k} P_{ijk}$$

$$u_i^{diff} = \tfrac{1}{2}\left(u_i^{UP} - u_i^{DOWN}\right) = \sum_j Q_{ij} v_j \Big/ \sum_j P_{ij}$$

$$v_j = \sum_j Q_{ji}^{-1} u_i^{diff} \sum_{j'} P_{ij'}$$

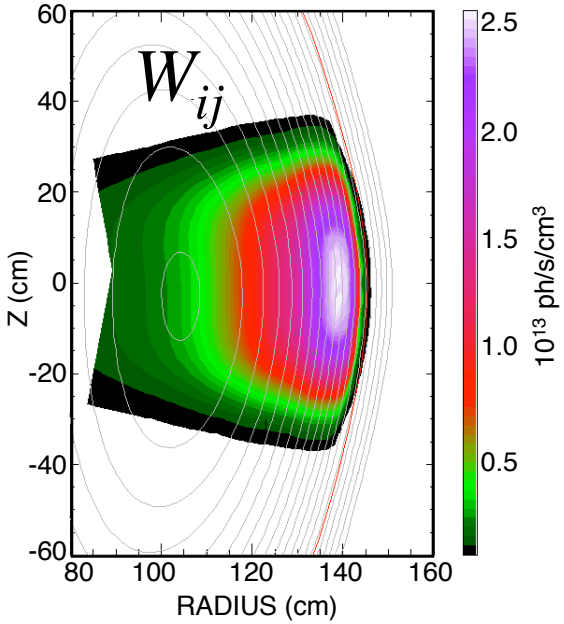

- The Charge Exchange emission varies along the line of sight (i)
- Midplane profiles of local T_e, N_e, T_i, V_ϕ, N_c are mapped into 2D using EFIT equilibrium
- A 2D beam attenuation gives N_{beam} vs zone (j) and height (k) in the plane of measurement
- A weight matrix based on computed CX emission is used to construct inversion matrices
  (atomic physics used here!)
- Local velocity inversion uses differential velocity, which removes non-poloidal velocity components

Comparison to Neoclassical Theory utilizes NCLASS and GTC-Neo

- NCLASS code
  - Calculates neoclassical transport properties of a multi-species axisymmetric plasma of arbitrary aspect ratio, geometry and collisionality
  - Module in TRANSP, separate post processor
- GTC-Neo code
  - δf particle-in-cell (PIC) code, allowing nonstandard orbits near the magnetic axis
  - Includes finite-orbit-width (banana width) effects
  - Calculated fluxes are "nonlocal" relative to the driving density and temperature gradients, with additional nonlocal smoothing over banana-width scale
  - GTC-Neo has been recently upgraded to handle impurity species
  - Utilizes same diagnostic information as TRANSP
- Expectations from neoclassical theory
  - $v_\theta \propto \nabla T_i/B$ *(both main ion and impurity ion)*
  - Sign of v_θ will change with sign of B_ϕ
  - Impurity v_θ also depends on ∇P *of main ion*

Local values of v_θ computed using matrix inversion

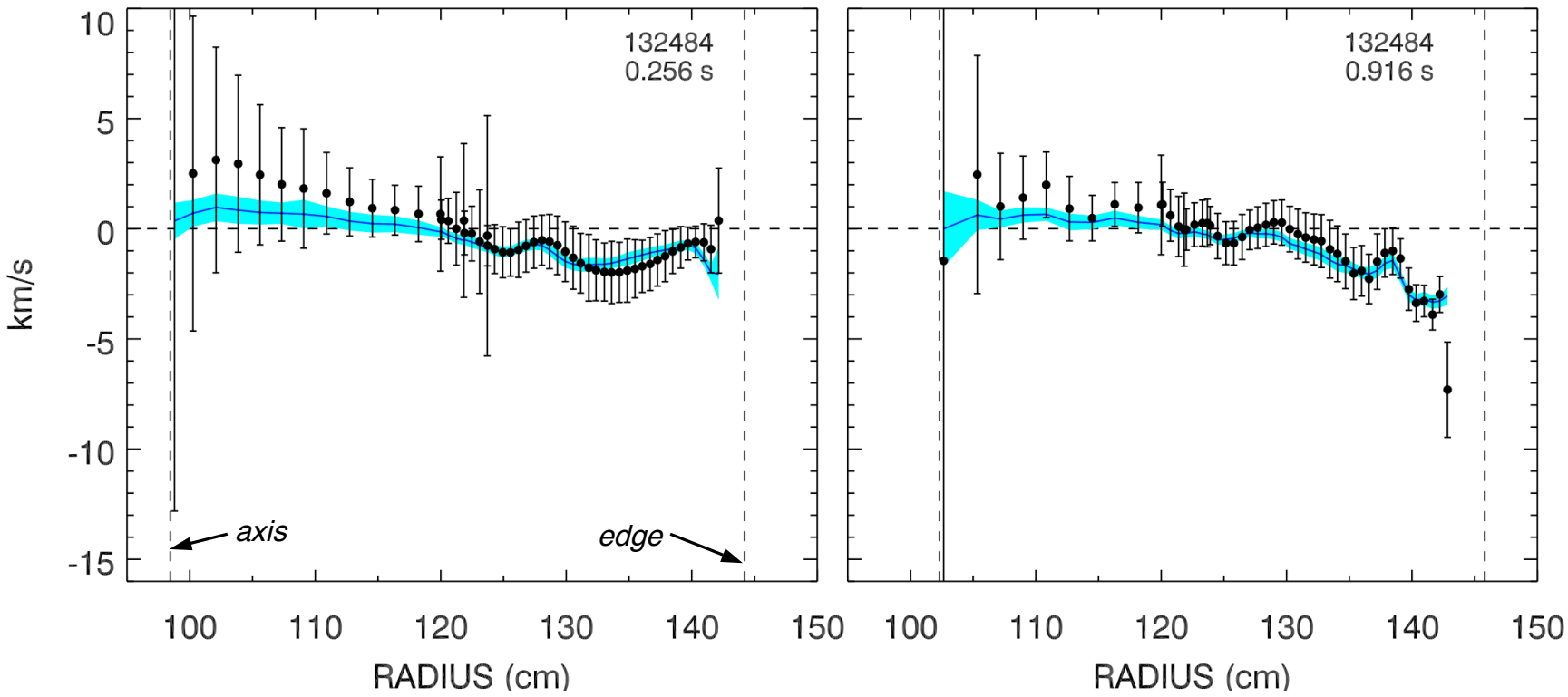

- Local poloidal velocity determined from inversion is similar to line-integrated velocity
- Central v_θ nearly constant, so line-integral is similar though radial smearing is large

Comparison of measured and neoclassical poloidal velocity profiles

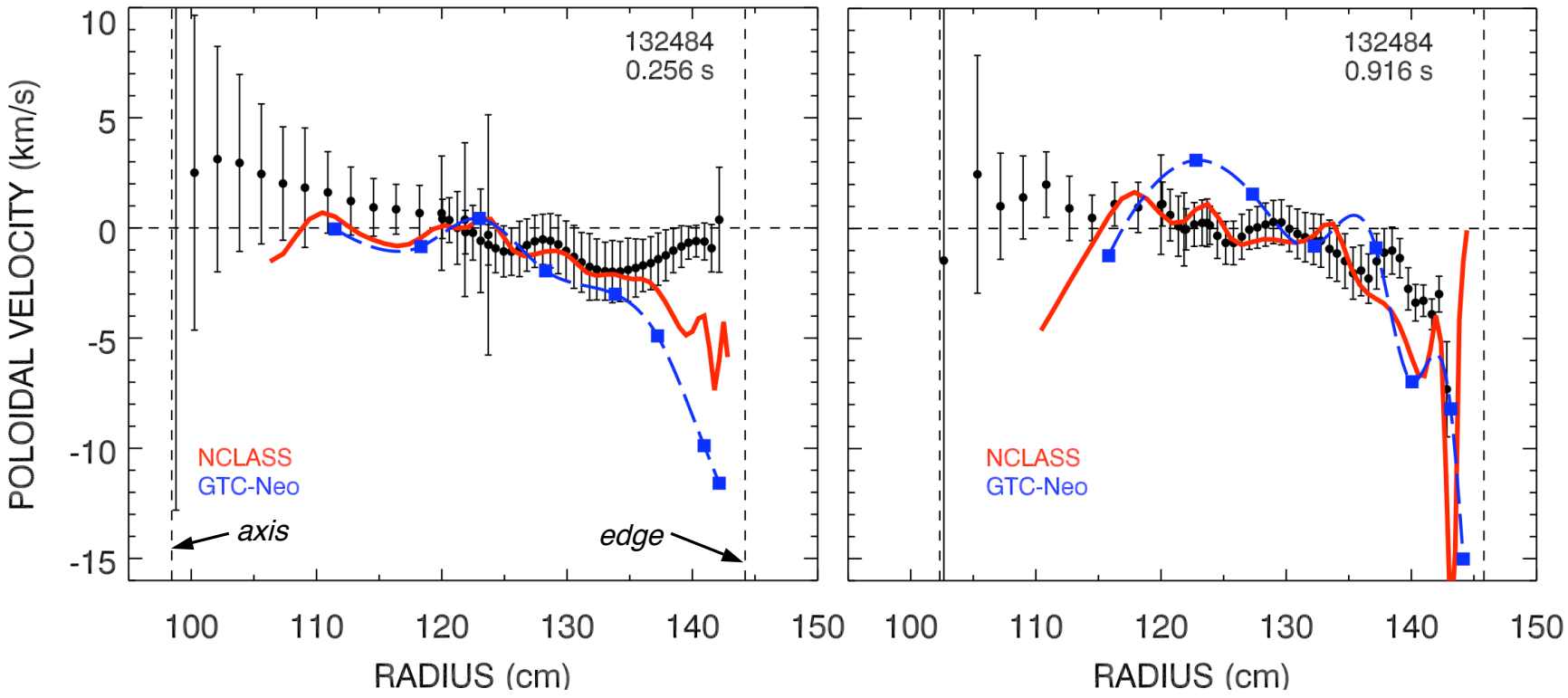

- Mixed agreement between measurement and theory vs. radius, time
- Measured v_θ consistent with neoclassical v_θ for inner core
- Large neoclassical v_θ at edge not seen in measured v_θ at early time
- More agreement between NCLASS and GTC-Neo for later time

Direction of v_θ should change with sign of B_ϕ consistent with Neoclassical Theory

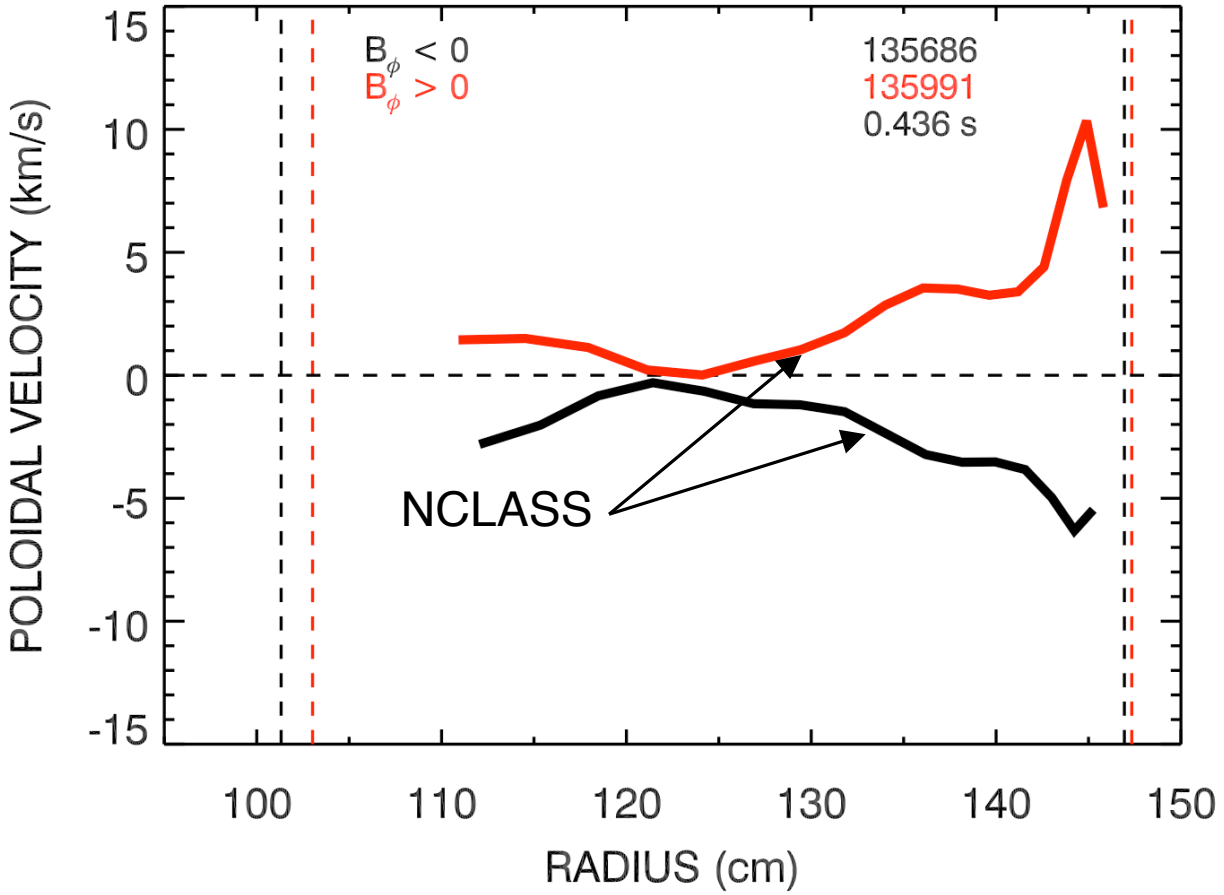

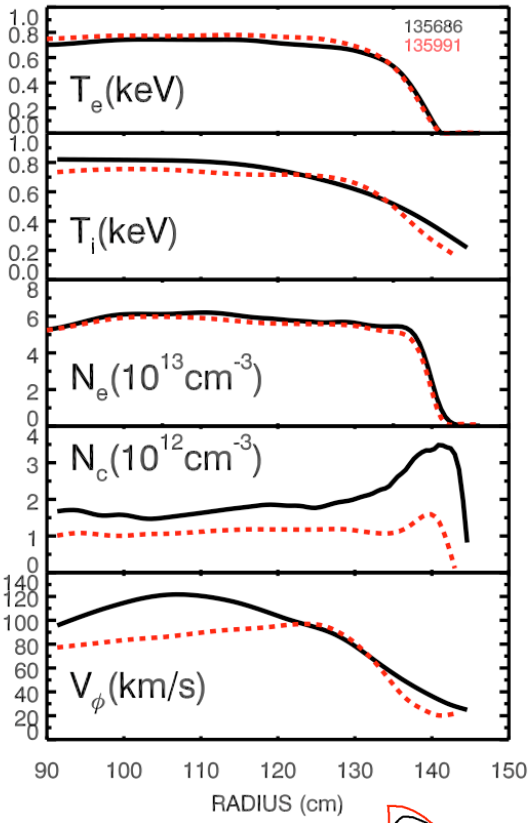

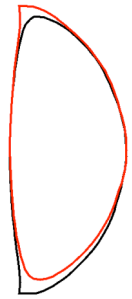

- Two similar discharges with opposite sign of B_ϕ compared
- NCLASS v_θ expectation from matched discharges straddles v_θ=0

Direction of v_θ should change with sign of B_ϕ consistent with Neoclassical Theory

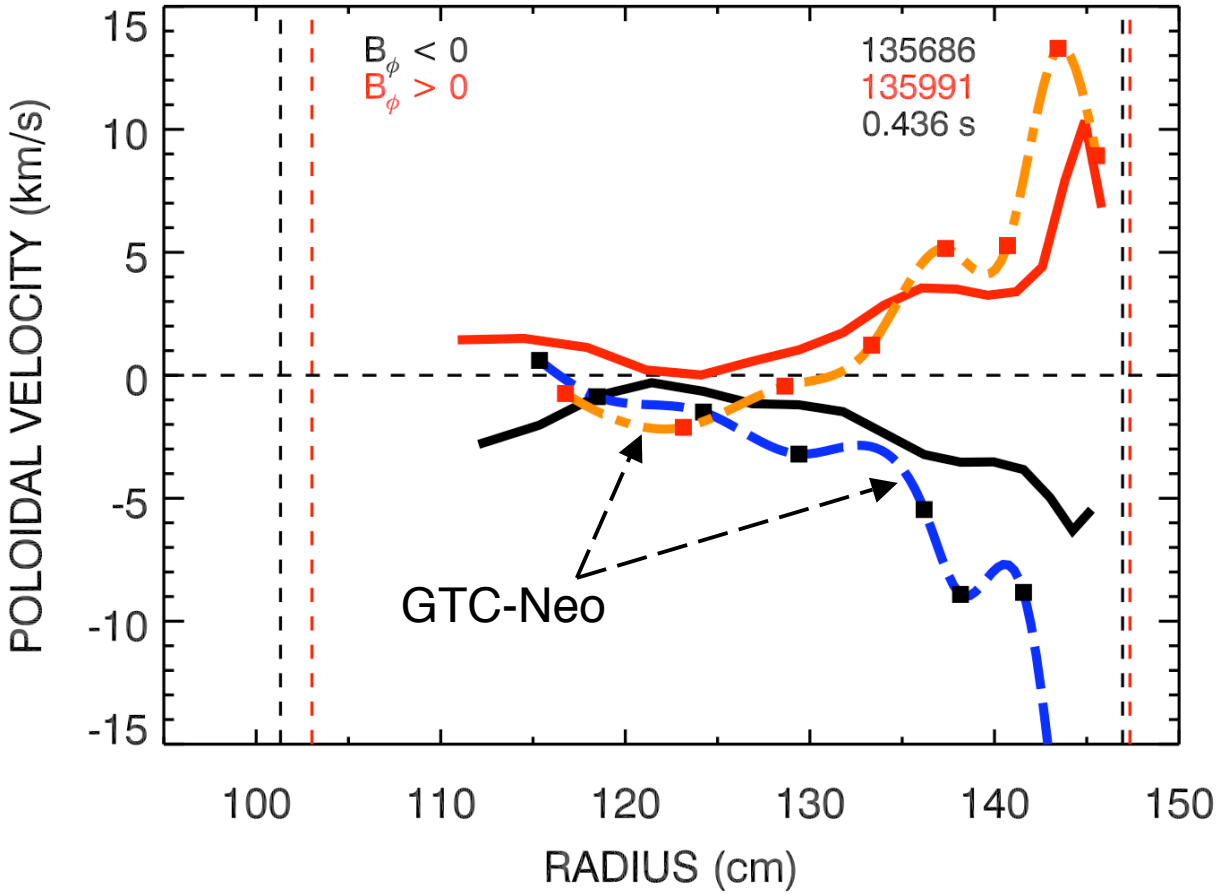

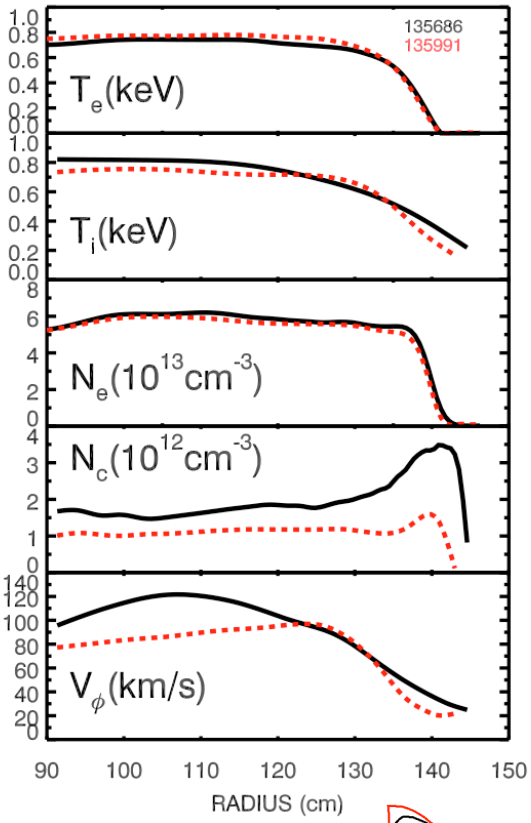

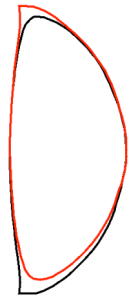

- GTC-Neo also shows similar sign change in v_θ expectation

Measured v_θ changes direction with sign of B_ϕ consistent with Neoclassical Theory

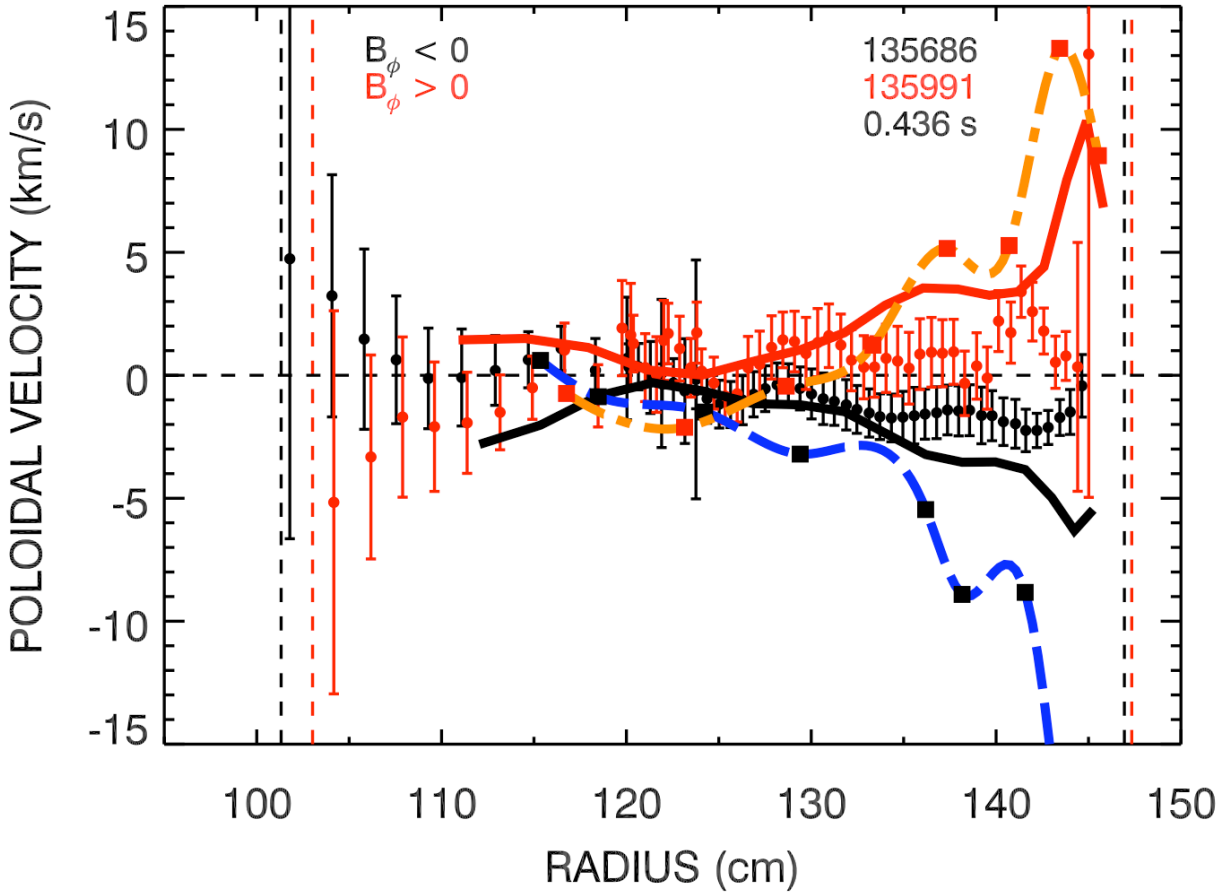

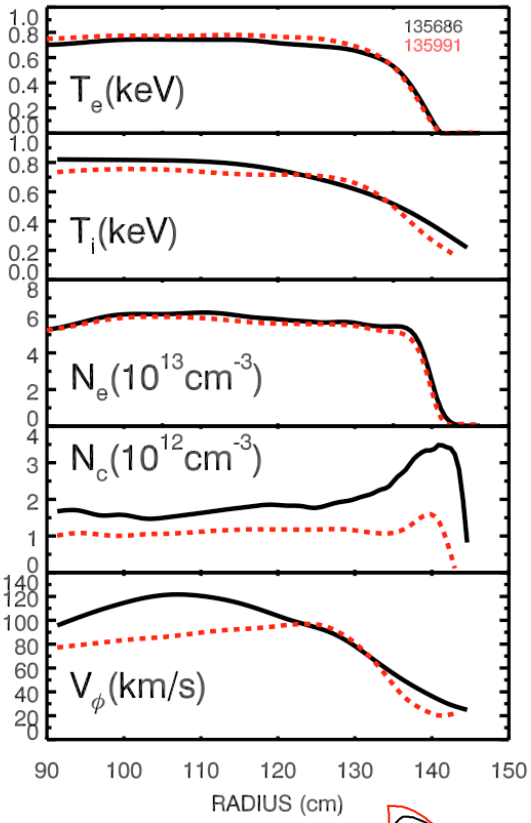

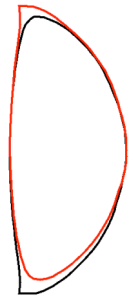

- Measured v_θ shows expected change in sign with reversal of B_ϕ
- *Measured v_θ consistently lower in magnitude than neoclassical v_θ*

Systematic variation in Poloidal Velocity observed as I_p and B_ϕ are varied

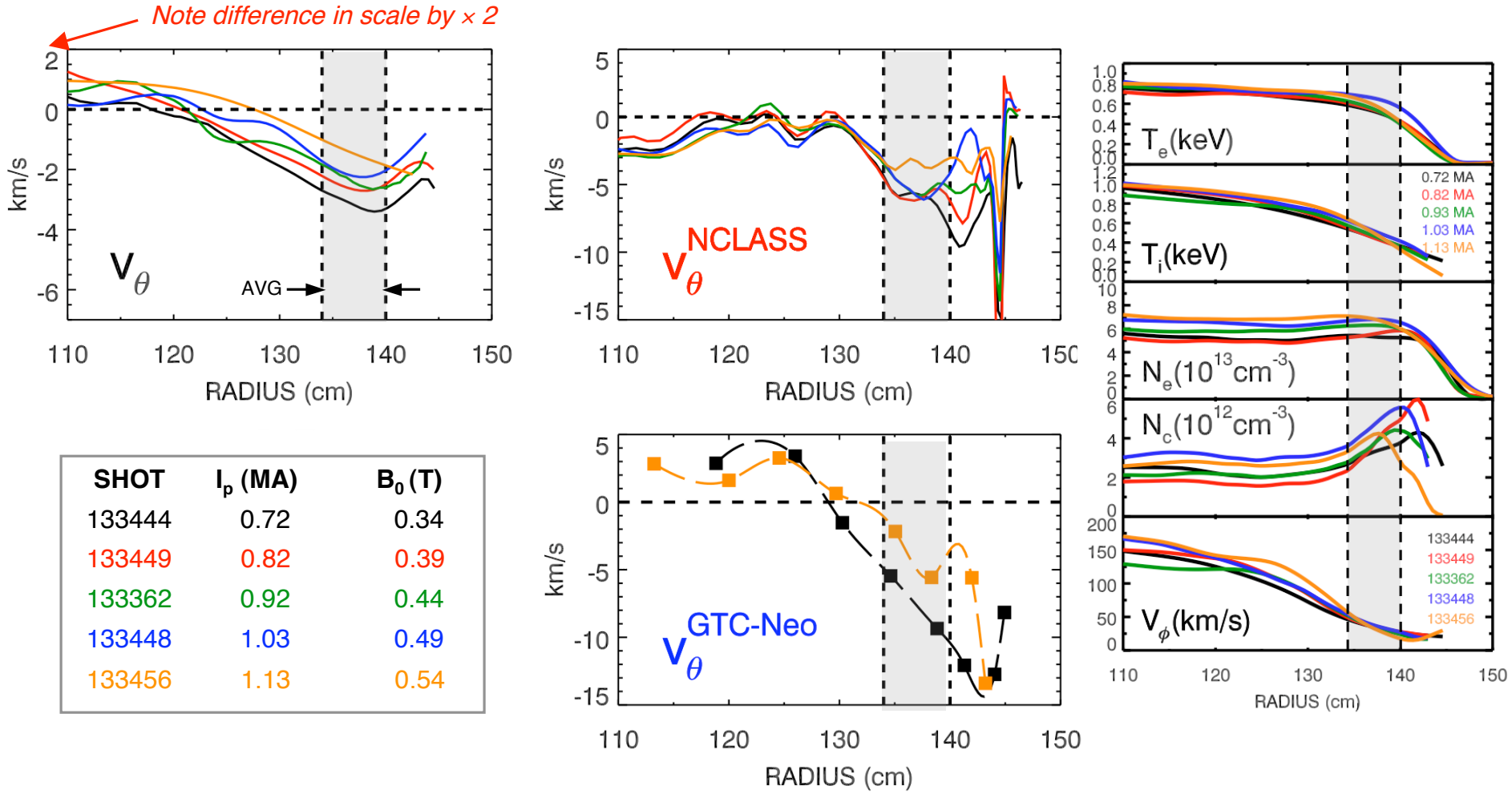

SHOT	I_p (MA)	B_0 (T)
133444	0.72	0.34
133449	0.82	0.39
133362	0.92	0.44
133448	1.03	0.49
133456	1.13	0.54

- I_p varied 0.7-1.1 MA with constant I_p/B_ϕ over several discharges
- *Take mean v_θ over range of radii to infer any trends*

Measurable trend in mean v_θ as I_p and B_ϕ are varied

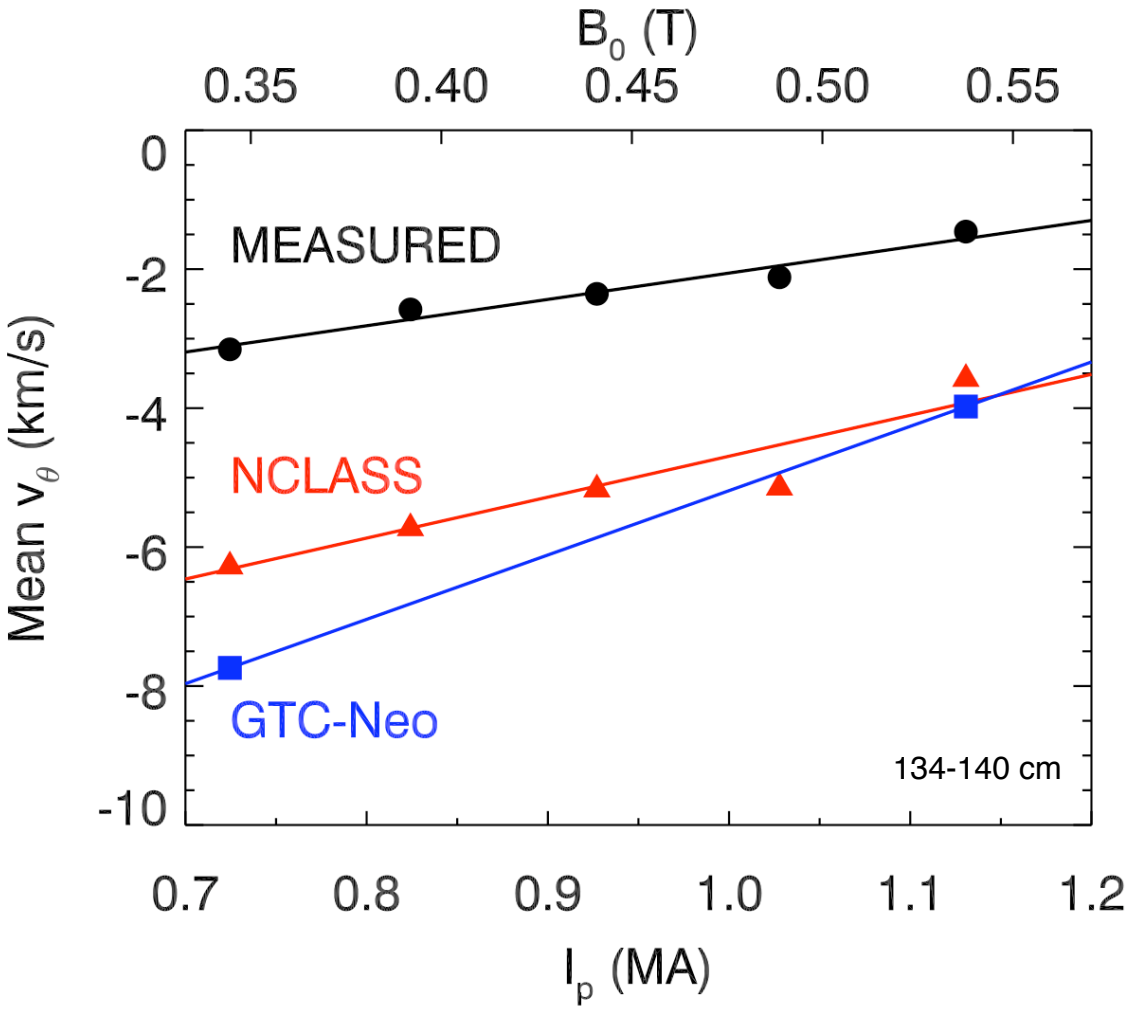

- Measured mean v_θ magnitude consistently less than neoclassical v_θ
- Similar differential behavior in neoclassical and measured v_θ
- Is this trend due to expected increase in magnitude of v_θ as *B?*
- T_i gradient increasing with I_p, while v_θ amplitude decreasing

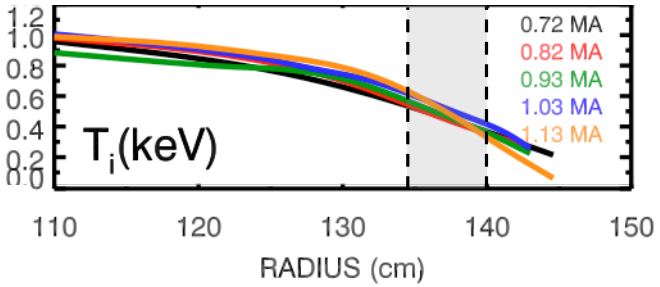

Radial Electric Field computed using all terms of Force Balance Equation

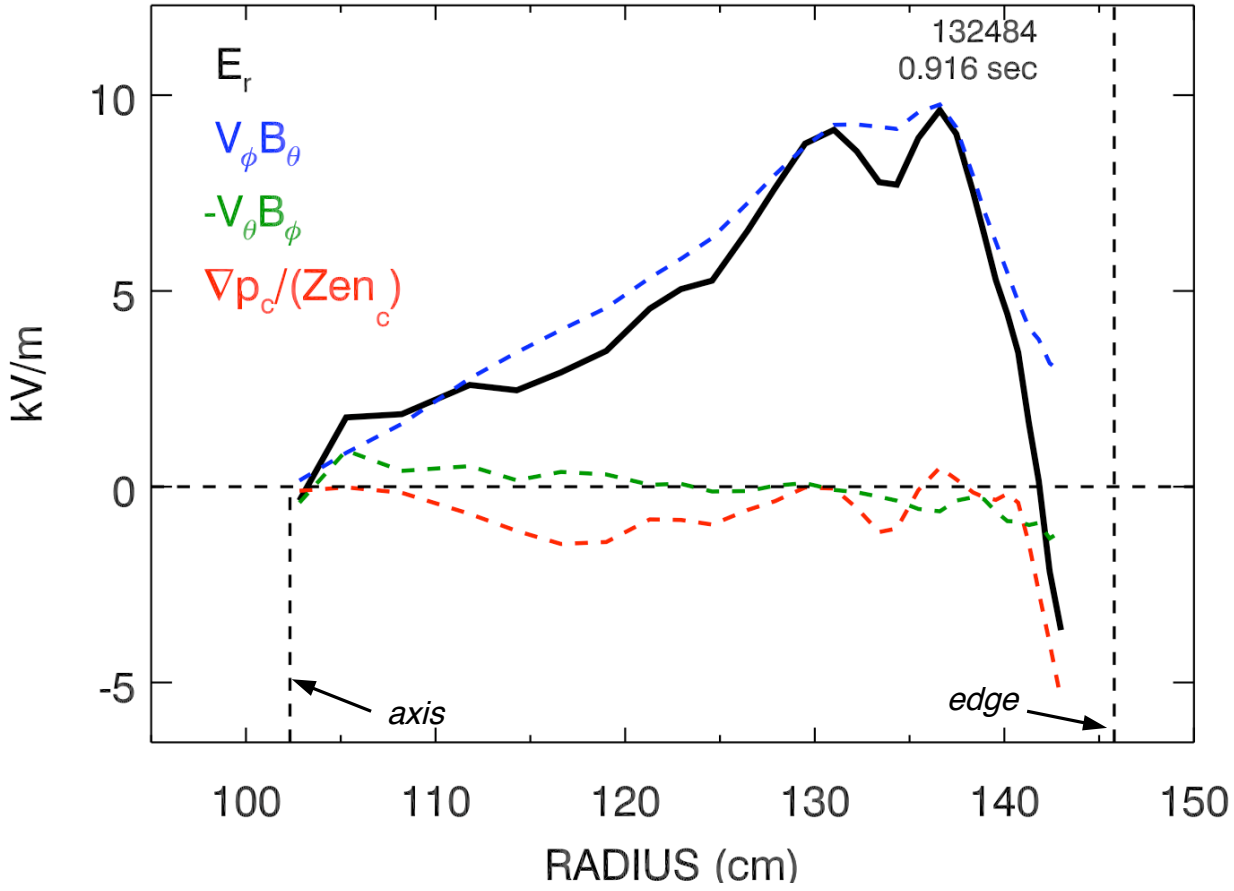

Force Balance Equation:

$$E_r = v_{\phi i} B_\theta - v_{\theta i} B_\phi + \frac{\nabla p_i}{e Z_i n_i}$$

- Small contribution to E_r due to poloidal velocity term
- Resolution of E_r near edge may be done with passive views

Measured Radial Electric Field consistent with Neoclassical Expectation

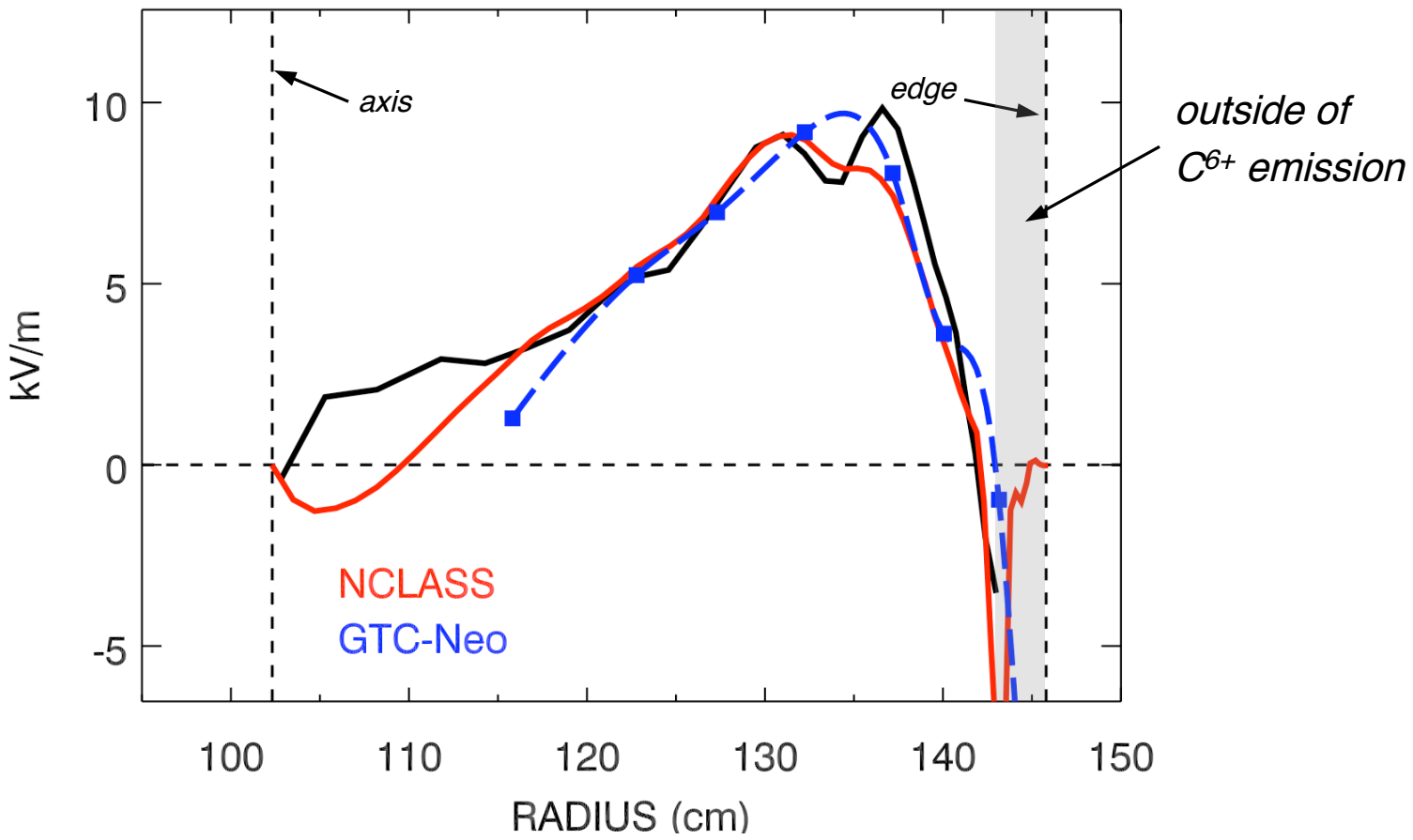

- E_r from NCLASS and GTC-Neo similar to measured E_r in core region
- Strong gradients in E_r just outside of C^{6+} emission region not well determined
- Passive emission from C^{5+} and C^{2+} could extend E_r profile to edge

Summary

- A new diagnostic provides poloidal velocity profiles on NSTX avoiding many atomic physics issues
- Magnitude *and* direction of measured v_θ consistent with neoclassical expectation on NSTX (also seen on MAST, differs on JET, DIII-D)
- Measured $v_\theta \leq v_\theta^{neoclassical}$ (within a factor of ~2)
- E_r determined using all terms of Force Balance Equation, $v_\theta B_\phi$ term small in NSTX
- Measured E_r is consistent with neoclassical in core
- More work required to evaluate E_r near edge, may be possible using passive C^{5+} emission
- Need to look for mechanisms for damping poloidal flow